Laboratory Observations of Cloud–Clear Air Mixing at Small Scales

SZYMON P. MALINOWSKI

University of Warsaw, Warsaw, Poland

ISZTAR ZAWADZKI

McGill University, Montreal, Quebec, Canada

PIOTR BANAT

University of Warsaw, Warsaw, Poland

21 November 1996 and 18 September 1997

ABSTRACT

Cloud–clear air mixing at scales from 1 mm to 1 m is observed in a laboratory chamber. Cross sections through the volume in which the mixing takes place are obtained by illuminating a planar sheet of cloud with laser light ($\lambda = 0.488$ μm, 1.2-mm thickness); the light is scattered by cloud droplets and photographed. Images indicate that complicated filament-like structures are created during mixing. Due to the properties of Mie scattering, this technique is in principle more sensitive to the larger cloud drops, and volumes with the small droplets may be underrepresented in the images. After digitization of the images, an interface between cloudy and clear-air filaments is investigated. Preliminary results indicate that at the scale of 2 cm the nature of the interface changes: at larger scales it exhibits self-similar properties, whereas at smaller scales it has a simple geometrical structure.

1. Introduction

The influence of mixing on cloud dynamics and microphysics has been a subject of interest since the early days of cloud physics. It has recently been advanced that mixing at very small scales may be important for microphysics (Grabowski 1993) or even large-scale dynamics (Haman and Pawlowska 1995). The link between the processes is suggested by theoretical considerations and by numerical simulations of turbulent mixing. However, direct observation of small-scale mixing in natural conditions is still not within experimental capabilities. The development of aircraft-mounted, cloud-droplet-sizing devices or thermodynamic sensors (e.g., Brenguier 1993; Baumgardner et al. 1993; Haman et al. 1997) is progressing rapidly, but it will take years to obtain fully dependable measurements at scales of the order of 1 cm or less. It seems that at this stage the most reasonable way to study small-scale mixing in clouds is in a laboratory environment.

A number of experiments investigating turbulent mixing at small scales are described in the literature (e.g., Dimotakis et al. 1983; Prasad and Sreenivasan 1990). Visualization techniques, such as the laser-induced fluorescence, allow observations of turbulent mixing of passive scalars down to Kolmogorov and Batchelor scales. These observations resulted in a new approach to turbulence and turbulent mixing, based on concepts of fractals and multifractals [see review in Sreenivasan (1991)]. A few attempts to apply a fractal description to the observed cloud structure have been made (Malinowski and Zawadzki 1993; Malinowski et al. 1994). They show that important differences between the turbulent mixing of passive scalars and mixing of cloudy air with clear air exist. The most plausible explanation of these differences is the active role of cloud droplets during mixing—that is, their evaporation—and the resulting cooling at the cloud–clear air interface, as well as the additional cloud transport by droplet sedimentation. To properly understand this problem, observations of small scales of mixing are required. As stated above, these cannot yet be studied from an aircraft. On the other hand, typical laboratory investigations of mixing using reacting fluids (e.g., Broadwell and Breidenthal 1982) can hardly reflect cloud conditions. Although cooling due to evaporation may be modeled by certain endothermic chemical reactions, the sedimentation of droplets is not taken into account in this approach. The importance of sedimentation that depends on the ori-

Corresponding author address: Dr. Szymon P. Malinowski, Institute of Geophysics, University of Warsaw, ul. Pasteura 7, Warsaw, PL-02-093, Poland.
E-mail: malina@mimuw.edu.pl

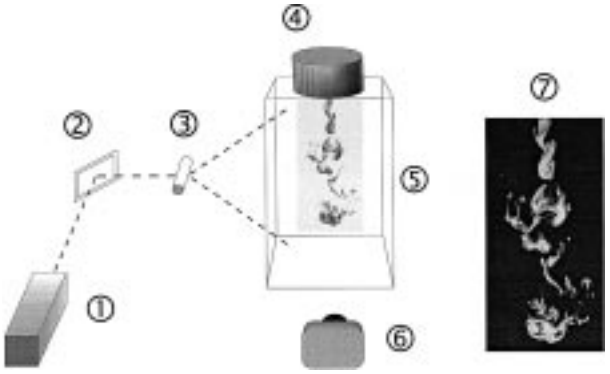

FIG. 1. A schematic view of the experimental setup: 1) laser, 2) mirror, 3) cylindrical lenses, 4) small chamber with the droplet generator, 5) main experimental chamber, 6) camera, and 7) an image of a cross section through a cloud undergoing mixing.

entation of the interface was shown by Grabowski (1993) in a numerical experiment.

In this paper we describe a new experimental approach that enables the investigation of turbulent mixing in clouds at scales from tens of centimeters down to millimeters. The technique to visualize the cloud–clear air interface makes use of laser sheet photography in a special cloud chamber. The experiment is described in section 2. First results are presented and discussed in section 3. Discussion and suggestions for the future can be found in section 4.

2. The experiment

Mixing takes place in a chamber 1 m deep, 1 m wide, and 1.8 m high (Fig. 1), which is fitted with a thermometer and a psychrometer to measure initial conditions of the environment. The second, smaller chamber, also fitted with a thermometer, is placed above the main one. An ultrasonic droplet generator (a commercially available ultrasonic humidifier) produces droplets that are blown into the small chamber. When the smaller chamber is full of mist (air between droplets is assumed to be saturated), the partition between chambers is opened. The weight of liquid water provides the initial negative buoyancy to the ''cloudy'' plume descending down to the large chamber and mixing with the ''environmental'' air. The initial diameter of the plume can be changed by modifying the size and shape of the opening. The velocity of the plume at the outlet was measured with a pressure velometer for a typical experimental setup; however, to avoid flow disturbances, it was not measured during the visualization experiments.

The estimated liquid water content (LWC) in the upper chamber (based on the efficiency of the droplet generator) is in the range of 3–15 g m^{-3}, depending on the time allowed for the generation of droplets. The droplet size distribution was measured by collecting droplets on a Vaseline-coated glass slide that was covered with a film of oil [for the description of this technique, see Zajcev and Ledochowich (1970)] and then photographing them with a microscope. A typical spectrum is shown in Fig. 2a.

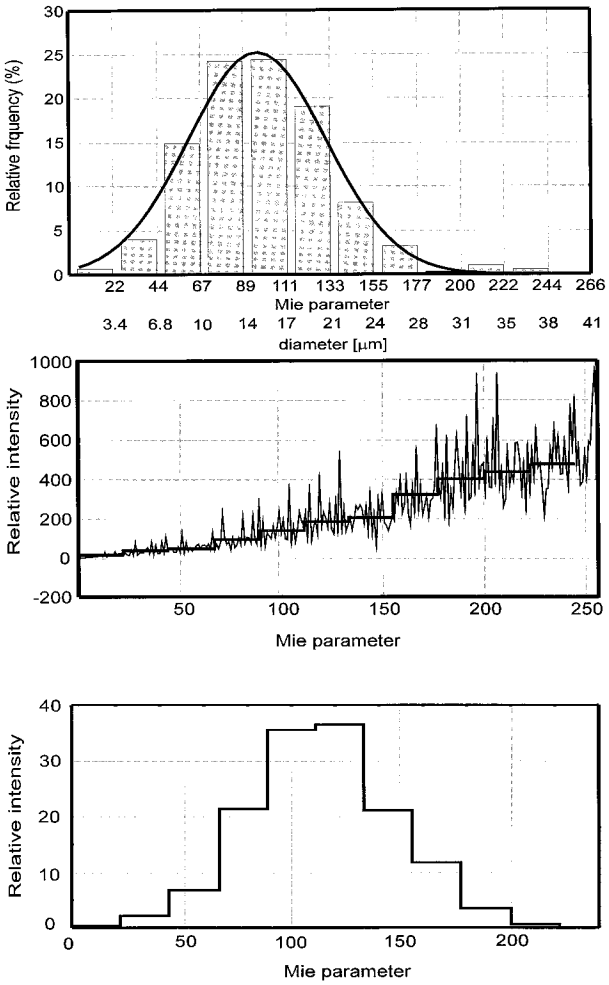

FIG. 2. (a) Typical observed droplet spectrum. (b) Intensity of the Mie scattering at 90° in the function of the Mie parameter calculated with a 2-m resolution and averaged on bins as in (a). (c) Effect of the droplet spectra on the intensity of scattered light at a 90° angle.

Cross sections through the volume in which mixing takes place are obtained by illuminating a planar sheet of cloud with laser light that is scattered by cloud droplets. The image is photographed or videotaped and then digitized and numerically processed.

a. Details of the experimental setup

The source of light in the experiment is an argon ion laser (wavelength 0.488 μm) with 2-W output in a 1.2-mm diameter beam. With a set of cylindrical lenses the laser beam is transformed, diverging with an angular width of 60° in vertical and remaining of 1.2-mm thickness. The uniformity of the intensity of the light in the

area of the observations is within ±15% of the mean value.

To obtain good quality photographs and videos, the light sheet has to illuminate the focal plane of the camera. This means that the optical axis of the camera must be perpendicular to the light plane, and therefore, the images that are taken correspond to the 90° Mie scattering by the cloud droplets. At this angle, Mie scattering is ineffective; that is, not much light is available. Long time exposures cannot be used to observe small-scale features of turbulence since dynamic structures observed during mixing often have characteristic velocities exceeding 10 cm s^{-1}. Thus, to obtain image resolution of about 1 mm (corresponding to the thickness of the light sheet, which limits the maximum available resolution), an exposure time of 0.01 s or smaller is necessary. A 35-mm camera equipped with a lens that has a focal ratio of $f/1.2$–$f/1.4$ and a focal length of 50 mm, placed at about 1.2 m from the plane of the light sheet, gives a reasonable quality photograph in typical experimental conditions with a film speed of 25 000 ASA or more. Kodak T-MAX P3200 film, pushed during processing to 25 000 ASA, was used. The negatives were digitized with a resolution of 1024 × 1535 pixels as gray-scale images with 8 bits (256 levels) of intensity. The resulting files were recorded on a CD-ROM for further digital processing.

A couple experimental runs were recorded with the use of a charge-coupled device (CCD) camera. CCD cameras may be more sensitive to light than other photographic media. A new experimental setup that uses a high-resolution video camera that allows for real-time digitization and storage of images is under development.

b. Scattering analysis

The width of each bin (3.45 μm) of the histogram of the droplet spectrum in Fig. 2a is larger than the error in the diameter of the individual droplet. The normal distribution curve estimated from this histogram has a maximum at a diameter of $d(y_{max}) = 14.9$ μm with a standard deviation of 5.5 μm. For the wavelength $\lambda = 0.488$ μm, $d(y_{max})$ corresponds to a Mie parameter value, $M = \pi d/\lambda$ (d is the droplet diameter), of 96.1, where, assuming spherical droplets, the Mie theory is suitable for describing the scattering.

Individual droplets are not resolved on images from the experiment. The maximum grain size of the negative corresponds to about 1 mm in physical space. Droplet concentration in the experiment has not been measured; however, we expect it to be a few drops per 1 mm^3. This means that the averaging, due to the grainy structure of the image, smooths the intensity fluctuations of the scattered light. Results of averaging on the Mie-scattering curve (bins equal to the bins from the histogram in Fig. 2a) are shown in Fig. 2b. Figure 2c presents the relative contributions of the intensity from the relative number of drops in each bin of the droplet spectrum. The best-fit Gaussian bell to this histogram has a maximum at $M = 112.5$ and a standard deviation of 34.0M. This indicates that in the images from the cloud chamber the most visible droplets have diameters in the range of 13.7–22.7 μm (M from 88.5 to 146.5). The observed ''shift'' to larger diameters (as compared to Fig. 2a) is due to the increase of the averaged scattering efficiency with the droplet diameter. This factor limits our capability to study the evolution of the cloud–clear air interface defined of the partially evaporated droplets of decreased diameter.

c. Image processing and products

The relationship between the brightness of each image pixel and the corresponding intensity of the scattered light is uncertain. Film processing is strongly nonlinear and not fully controllable. Results may vary from roll to roll and from scene to scene in the same roll of film. Quantitative analysis of the image to obtain information about droplet spectra is impossible. However, information on the location of the interface between cloudy and clear air can be extracted from data with good results. This interface is defined by a certain threshold of image brightness. Discussion of the effect of the value of the threshold on results will be given later.

3. Preliminary results

a. First images

The example of an image from the first successful experiment is presented in Fig. 3. The photograph shows mature stages of mixing of the free-falling negatively buoyant plume entering the large chamber through a circular opening 10 cm in diameter. Such structures have been observed at tens of seconds after closing the diaphragm between the large and small chambers. The spiral patterns are cross sections through the stretched vortex tubes—regions where strong dissipation of the turbulent energy is very likely.

b. An investigation of the cloud–clear air interface

Figure 4 is a segment of a processed image with the extracted interface between cloudy and clear-air filaments, given by a certain intensity threshold. The box-counting method (see, e.g., Falconer 1990) was applied to the interface in order to investigate its scaling properties [as in Sreenivasan et al. (1989), Malinowski and Zawadzki (1993), and Malinowski et al. (1994)]. The final result for 17 snapshots with well-developed filamentation of the cloudy volumes (as in Figs. 3 and 4) is shown in Fig. 5a. The sharp change of the box dimension (slope on the log-log plot) from about 1 at small scales to about 7/5 in scales above 2 cm is its key feature. The robustness of this break has been tested by com-

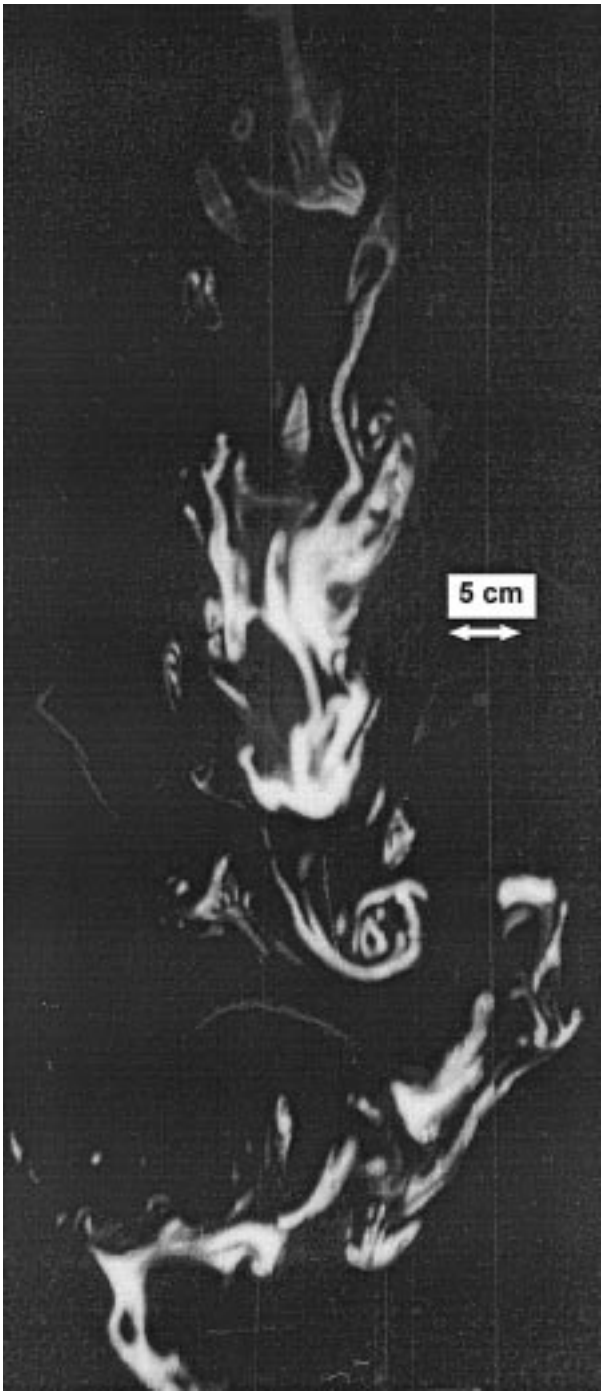

FIG. 3. An example of the cross section through the developed mixing in a negatively buoyant plume (free flow of the plume by opening the 10-cm diameter).

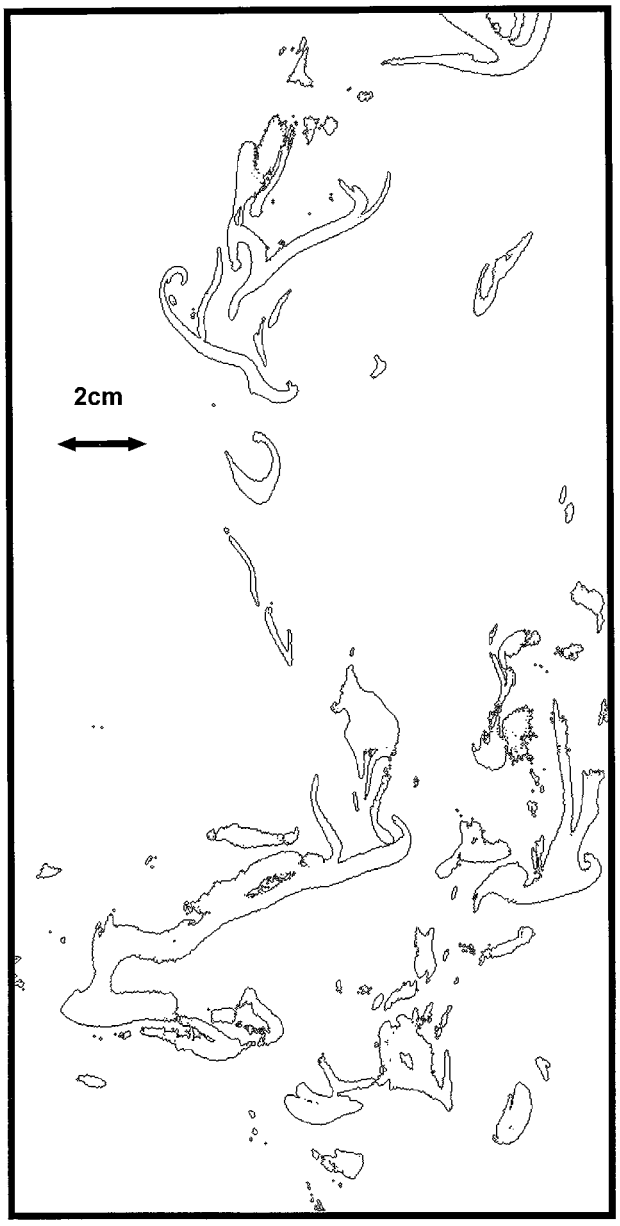

FIG. 4. An example of the interface between cloud and clear air extracted from the experimental image.

paring the Pearson correlations for cases of simple linear regression to cases of two-line regression. A one-sided test of the Pearson correlations gives acceptance to the hypothesis that two-line regression is better than one-line regression on the confidence level of 0.95 for the intensity threshold 40, and 0.92 for the intensity threshold 70.

The break in scaling and the values of the slopes in each range of scales mean that at scales below 2 cm the interface is simply a geometrical one, while at larger scales it has a noninteger dimension of the value closer to 1.36, as reported for passive scalars by Sreenivasan et al. (1989), than to 1.55, as observed in clouds by Malinowski and Zawadzki (1993).

The sensitivity of the calculated box dimension to the value of the threshold for which the interface is defined is shown in Fig. 5b. For thresholds larger than 40 (out of 255 gray scale) the box dimension is weakly depen-

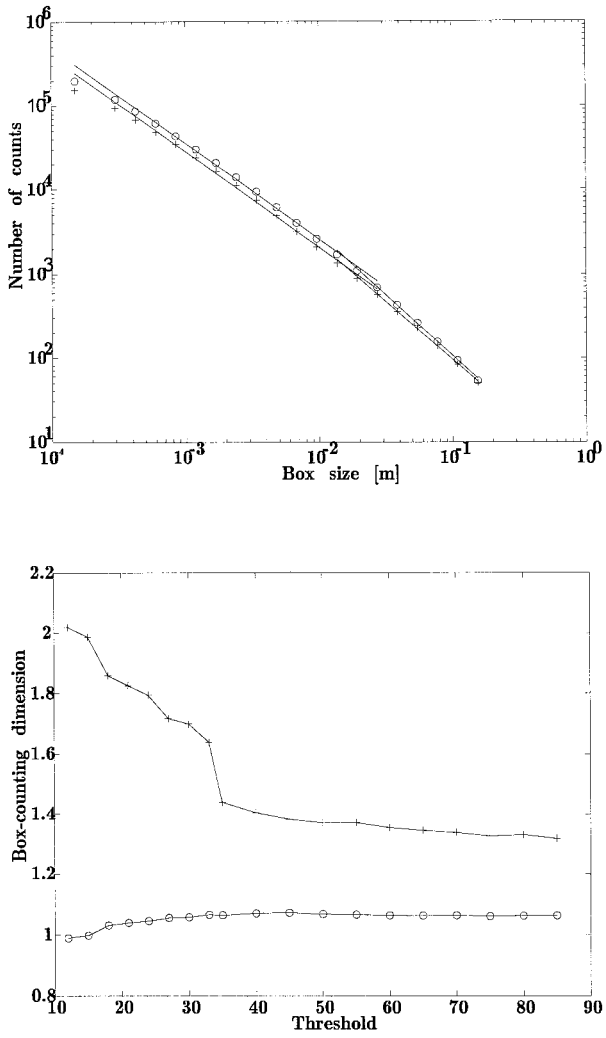

FIG. 5. (a) Box counting on a cloud–clear air interface, sum for 11 independent snapshots. The circles correspond to the interface obtained for threshold 40 (out of 255 gray levels), and the crosses for threshold 70. The error bars are omitted on the plot since their maximum size is smaller than the size of the circles and crosses. (b) The dependence of the box-counting dimension on the intensity threshold. The upper plot shows the dimension calculated for scales above 2 cm, and the lower plot for scales below 2 cm.

dent on the threshold value. Thus, despite all of the uncertainties concerning imaging and chemical processing of the film, the break of the scaling behavior around 2 cm is well defined. This mixing behavior is different from the one observed in laboratory flows with passive scalars, in which the scaling behavior was well established down to the scale of 2η (two Kolmogorov scales) (Sreenivasan et al. 1989). In our case, the upper limit of the Kolmogorov scale may be estimated assuming the characteristic velocity of $V = 0.1$ m s^{-1} for the plume entering the large chamber through the opening of radius $r = 0.05$ m. These values give shear estimates of $S \approx V/r = 2$ s^{-1}. The dissipation rate of turbulent kinetic energy may be then estimated as $\varepsilon = \nu S^2$, and the Kolmogorov scale as $\eta = (\nu^3/\varepsilon)^{1/4}$. Substituting $\nu = 1.5 \times 10^{-5}$ m^2 s^{-1}, we get $2\eta \approx 5$ mm, which is four times less than the break in scaling. The real values of ε should be larger, due to the larger values of shear, than the assumed minimum and the possible production of turbulence in small scales due to evaporation of droplets at the interface and the resulting production of turbulence by buoyancy.

4. Summary

Results presented above show that it is possible to observe directly in the laboratory small scales of cloud–clear air mixing. The smallest observed structures are the order of millimeters, a limitation set by the maximum speed of the photographs, for which a sufficient amount of the scattered light was available, as well as by the grain size of the film. The largest scales are limited by the size of the cloud chamber and are of the order of 1 m. These are scales at which the interaction between dynamics and microphysics takes place.

The experimental setup is being modified to remove its weaknesses. The primary goal now is to measure the LWC of the plume entering the cloud chamber as well as to improve the imaging procedure. However, despite the relatively primitive experimental setup, preliminary results already look very interesting. The break in scaling properties around 2 cm indicates that turbulence in clouds is not self-similar down to the Kolmogorov scale. It is likely that the size-dependent droplet sedimentation destroys the scale-invariant structure resulting from the turbulence created by evaporative cooling and shear. The 2-cm scale would then result from the equilibrium between the rate at which the scale invariance is produced by turbulence and the rate at which sedimentation makes uniform the droplet distribution in space. It remains to be determined whether the scale at which the break occurs is dependent on conditions such as the clear-air humidity, LWC, the temperature in the cloud and its environment, etc.

The last remark concerns the value of the box-counting dimension in scales above 2 cm (about 1.4) and its inconsistency with values obtained by Malinowski and Zawadzki (1993) (about 0.55 on 1D horizontal cuts through clouds) and Malinowski et al. (1994) (0.44–0.62 and even to 0.95 on similar cuts). The reason for this inconsistency is uncertain; however, several explanations for this effect are possible.

1) Not all clouds can be characterized by a single value of the box-counting dimension. The particular value of the dimension may depend on the type and the characteristics of the individual clouds.
2) There exists some kind of anisotropy in clouds that cannot be investigated on 1D horizontal cuts. However, the anisotropy influences the box-counting dimension of the cloud–clear air interface.
3) In scales investigated in the described experiment

the dimension of the interface is larger than in scales investigated from an aircraft.

The authors believe that explanation 2 is true but that explanation 1 is also possible. The answer to this problem, however, requires more study of cloud properties, both in the cloud chamber and in natural conditions.

Acknowledgments. This research was sponsored by Grant 6 P201 055 05 of the Polish Committee for Scientific Research. The authors thank Dr. R. Balcer for his help in measuring the droplet spectrum.

REFERENCES

Baumgardner, D., B. Baker, and K. Weaver, 1993: A technique for the measurement of cloud structure on centimeter scales. *J. Atmos. Oceanic Technol.,* **10,** 557–565.

Brenguier, J. L., 1993: Observation of cloud structure at the centimeter scale. *J. Appl. Meteor.,* **32,** 783–793.

——, and W. Grabowski, 1993: Cumulus entrainment and cloud droplet spectra. A numerical model within a two-dimensional dynamical framework. *J. Atmos. Sci.,* **50,** 120–136.

Broadwell, J. E., and R. E. Breidenthal, 1982: A simple model of mixing and chemical reaction in a turbulent shear layer. *J. Fluid Mech.,* **125,** 397–410.

Dimotakis, P. E., R. C. M. Lye, and D. A. Papantoniou, 1983: Structure and dynamics of round turbulent jets. *Phys. Fluids,* **26,** 3185–3192.

Falconer, K., 1990: *Fractal Geometry. Mathematical Foundations and Applications.* Wiley & Sons, 288 pp.

Grabowski, W. W., 1993: Cumulus entrainment, fine scale mixing and buoyancy reversal. *Quart. J. Roy. Meteor. Soc.,* **119,** 935–956.

Haman, K. E., and H. Pawlowska, 1995: On the dynamics of nonactive parts of convective clouds. *J. Atmos. Sci.,* **52,** 519–531.

——, A. M. Makulski, S. P. Malinowski, and R. Busen, 1997: A new ultrafast thermometer for airborne measurements in clouds. *J. Atmos. Oceanic Technol.,* **14,** 217–227.

Malinowski, S. P., and I. Zawadzki, 1993: On the surface of clouds. *J. Atmos. Sci.,* **50,** 5–13.

——, M. Y. Leclerc, and D. Baumgardner, 1994: Fractal analysis of high-resolution cloud droplet measurements. *J. Atmos. Sci.,* **51,** 387–413.

Prasad, R. R., and K. R. Sreenivasan, 1990: The measurement and interpretation of fractal dimensions of surfaces in turbulent flows. *Phys. Fluids A,* **2,** 792–807.

Sreenivasan, K. R., 1991: Fractals and multifractals in fluid turbulence. *Annu. Rev. Fluid Mech.,* **23,** 539–600.

——, R. Ramshankar, and C. Meneveau, 1989: Mixing, entrainment and fractal dimension of surfaces in turbulent flow. *Proc. Roy. Soc. London A,* **421,** 79–108.

Zajcev, V. A., and A. A. Ledochowich, 1970: Pribory dla issledovanija tumanov i oblakov i izmerenija vlaznosti. *Gidrometeorologicheskoje Izdatelstvo,* 63–65.